Control de un sistema de tracción eléctrica por medio de regulación en esquema cascada y control vectorial

Dominguez, Xavier[1]; Pozo, Marcelo[1]; Ortega, Leonardo[1]

[1]*Escuela Politécnica Nacional, Facultad de Ingeniería Eléctrica y Electrónica, Quito, Ecuador*

Resumen: El propósito del presente artículo consiste en el control de un sistema de tracción eléctrica. En primer lugar se detalla el modo de funcionamiento del convertidor bidireccional DC-DC tipo medio puente empleado para este tipo de aplicaciones. Segundo, se propone un control del sistema bajo el esquema tipo cascada. Luego, por medio de un inversor trifásico de tres ramales que emplea una estrategia modulación, se realiza el control de torque y velocidad de una Máquina Sincrónica de Imanes Permanentes en Superficie (SPMSM) usando criterios de control vectorial. Los resultados obtenidos muestran respuestas exitosas tanto en régimen dinámico como estacionario en operación modo motor y modo regeneración de energía.

Palabras clave: Control en cascada, Control vectorial de Máquinas, Convertidor DC-DC bidireccional, SPMSM.

Control of an electric traction system by means of cascade scheme regulation and machine vector control

Abstract: The aim of this paper is the control of an electric traction system. Firstly, the operation of the half-bridge bidirectional DC-DC converter employed for this kind of applications is detailed. Secondly, the control of the system is proposed by using a cascade control scheme. Later, by means of a three-leg three-phase inverter that employs a pulse width modulation strategy, the torque and speed control is achieved for a Surface Permanent Magnet Synchronous Machine (SPMSM). Vector control is also used to achieve this goal. The results exhibit successful responses for both, dynamic and steady state, for operation in motor mode and energy regeneration mode.

Keywords: Bidirectional DC-DC converter, Cascade Control, Machine Vector Control, SPMSM.

1. INTRODUCTION

The use of an effective bidirectional power converter combined with modern energy storage systems and efficient electrical machines is a crucial aspect for the development of reliable electrically-powered traction applications. For these systems, to manage a double-way power flow, the use of a simple and robust DC-DC power converter plus an inverter is required. The converter that fulfills these features is a bidirectional non-isolated buck-boost type (Pillay et al, 1985) (Du et al, 2010) in one hand. And on the other hand, for the inverter, a three-leg three-phase topology having antiparallel diodes on each power switch has been considered. Therefore, these two power converters need to be effectively controlled to properly deliver energy from the battery to the electric machine when acting as a motor, and in the opposite case allowing to charge the battery by energy regeneration.

Depending on the speed-torque demand and profile of the electrical vehicle, the inverter has to supply the required voltage to the electric machine from the power converter.

In this study, due to its low inertia, high power density, controllability and outstanding efficiency; a Surface Permanent-Magnet Synchronous Machine (SPMSM) is used (Kitajima et al, 2014)(Maekawa et al, 2014). Consequently, to take advantage of these features and design a robust control scheme against load variations during motoring as well as regeneration modes, the development of a reliable and practical control strategy for the bidirectional DC-DC converter and also for the inverter is required; this is precisely the scope of this paper. This aim will be accomplished by the use of a nested control structure for the buck-boost bidirectional DC-DC converter and a vector control strategy for the SPMSM. The entire control logic was firstly validated by simulation and also via its digital upgrading in a commercial embedded system.

2. THE BUCK-BOOST BIDIRECTIONAL DC-DC CONVERTER

The overall components for electric vehicle applications are exposed in Figure 1 where the bidirectional power flows can be observed. This bidirectional power exchange is achieved by means of the bidirectional DC-DC power converter, whose topology is a buck-boost type, as it is shown in Figure

2. v_L represents the battery voltage, v_H the DC-link voltage, L and R denote the inductance and the internal resistance of the inductance respectively, R_H the inverter input impedance, and C_H is the DC-link capacitance. The two operation modes present opposite inductance current direction to achieve extraction or injection of energy from or to the low-voltage battery bank.
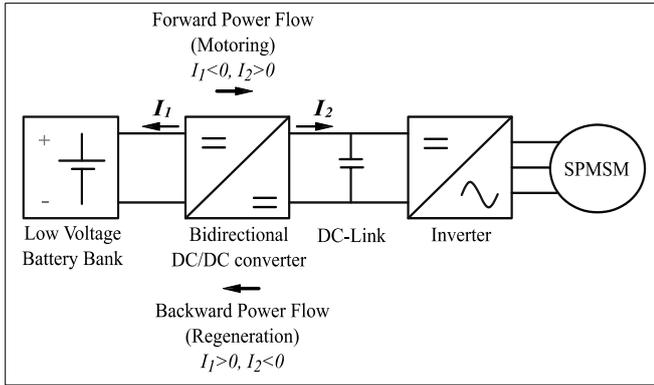

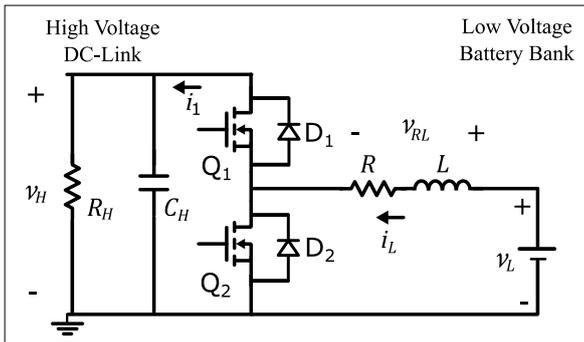**Figure 1**. General scheme for electric vehicle applications

Figure 2. Half-Bridge bidirectional DC-DC power converter

In this study, the unified current controller proposed by (Junhong et al, 2008) has been considered as the buck and boost modes have the same power plant. This approach relays on the opposite switching between switches Q1 and Q2. For the case of electric tractions applications, the major challenge for the DC-DC converter consists on regulating the high-voltage DC link provided that the low-voltage battery bank is a robust DC source that presents a relative slow discharge during normal operation. The ON and OFF states for the boost mode are shown in Figure 3.
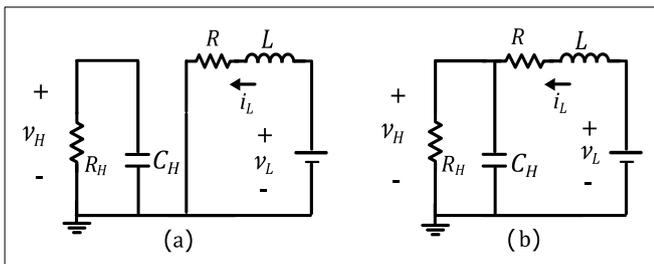

Figure 3. Boost operation: (a) ON state: Q₂ ON – Q₁ OFF, (b) OFF state: Q₂ OFF – Q₁ ON

Thus, the state-space equations for the ON and OFF states are described by (1)-(2):

$$\dot{x}(t) = A_{ON}\, x(t) + B_{ON}\, u(t)$$

$$\begin{pmatrix} \dot{i}_L \\ \dot{v}_H \end{pmatrix} = \begin{pmatrix} -\dfrac{R}{L} & 0 \\ 0 & -\dfrac{1}{C_H\, R_H} \end{pmatrix} \begin{pmatrix} i_L \\ v_H \end{pmatrix} + \begin{pmatrix} \dfrac{1}{L} \\ 0 \end{pmatrix} v_L \tag{1}$$

$$\dot{x}(t) = A_{OFF}\, x(t) + B_{OFF}\, u(t)$$

$$\begin{pmatrix} \dot{i}_L \\ \dot{v}_H \end{pmatrix} = \begin{pmatrix} \dfrac{-R}{L} & -\dfrac{1}{L} \\ \dfrac{1}{C_H} & -\dfrac{1}{C_H\, R_H} \end{pmatrix} \begin{pmatrix} i_L \\ v_H \end{pmatrix} + \begin{pmatrix} \dfrac{1}{L} \\ 0 \end{pmatrix} v_L \tag{2}$$

The average value of the previous equations can be expressed as (3)-(4):

$$A = D\, A_{ON} + (1-D)\, A_{OFF} = \begin{pmatrix} -\dfrac{R}{L} & -\dfrac{1-D}{L} \\ \dfrac{1-D}{C_H} & -\dfrac{1}{C_H\, R_H} \end{pmatrix} \tag{3}$$

$$B = D\, B_{ON} + (1-D)\, B_{OFF} = \begin{pmatrix} \dfrac{1}{L} \\ 0 \end{pmatrix} \tag{4}$$

where D represents the duty cycle of the pulse width modulation (PWM) on the power semiconductor. Finally, the state-space average equations (Erickson and Maksimovi, 2001) can be derived as detailed in (5):

$$\dot{x}(t) = A\, x(t) + B\, u(t)$$

$$\begin{pmatrix} \dot{i}_L \\ \dot{v}_H \end{pmatrix} = \begin{pmatrix} -\dfrac{R}{L} & \dfrac{-(1-D)}{L} \\ \dfrac{1-D}{C_H} & -\dfrac{1}{C_H R_H} \end{pmatrix} \begin{pmatrix} i_L \\ v_H \end{pmatrix} + \begin{pmatrix} \dfrac{1}{L} \\ 0 \end{pmatrix} v_L \tag{5}$$

As the DC-link voltage is controlled by means of the duty cycle, the understanding of the relationship between this variable and the other variables in steady state ($\dot{x} = 0$) is required as in (6)-(7):

$$0 = A\, x + B\, u \tag{6}$$

$$\begin{pmatrix} 0 \\ 0 \end{pmatrix} = \begin{pmatrix} -\dfrac{R}{L} & \dfrac{-(1-D)}{L} \\ \dfrac{1-D}{C_H} & -\dfrac{1}{C_H R_H} \end{pmatrix} \begin{pmatrix} i_L \\ v_H \end{pmatrix} + \begin{pmatrix} \dfrac{1}{L} \\ 0 \end{pmatrix} v_L \tag{7}$$

From the first line in Equation 7, (8) is obtained:

$$0 = \frac{-R}{L} i_L - \frac{-(1-D)}{L} v_H + \frac{1}{L} v_L \tag{8}$$

After simple mathematical treatment the duty cycle exhibited in (9) can be attained:

$$D = \frac{v_{RL} - v_L}{v_H} + 1 \tag{9}$$

Where v_{RL} denote the overall voltage on the inductor (across its inductance and internal resistance). As the duty cycle D is simultaneously related with the two state-variables (i_L and v_H), the system places in a non-minimum phase condition (Tarakanath et al, 2014) which involves control instabilities. Hence, a cascade control scheme (See Figure 4) with an outer voltage loop and an inner current loop is used as the inductor current presents a higher frequency bandwidth than the DC-link voltage frequency bandwidth.
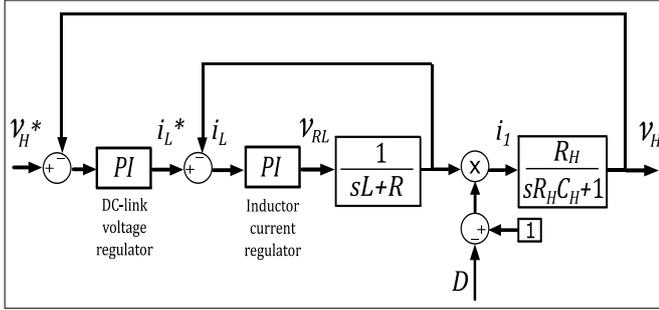

Figure 4. Cascade control for the bidirectional DC-DC power converter

For both, the outer and inner control loops, PI regulators are proposed. From Equations 10-13, the proportional (Kp) and integral-terms (Ti) for the outer voltage controller and the inner current controller have been designed to have a closed-loop bandwidth (BW) of 30[Hz] and 500[Hz] respectively. Using the pole-cancellation criterion, the controllers parameters can be estimated (Savaresi et al, 2010) by means of (10)-(13):

$$Kp_{outer} = 2\pi.BW_{outer}.C_H \qquad (10)$$

$$Ti_{outer} = R_H.C_H \qquad (11)$$

$$Kp_{inner} = 2\pi.BW_{inner}.L \qquad (12)$$

$$Ti_{inner} = L/R \qquad (13)$$

For the converter, $R = 0.5[\Omega]$, $C = 2000[\mu F]$, $L = 25[mH]$ and $v_L = 202[V]$ have been considered.

3. VECTOR CONTROL FOR THE SPMSM

Once the operation of the bidirectional converter has been discussed, the operation and control of the inverter and the traction machine are required. A three-phase two level inverter feeds the SPMSM (Figure 5).

Additionally, an external mechanical load directly coupled to the axis of the machine is used to operate in motoring and regeneration modes. The parameters of the SPMSM are shown in Table 1 at the Appendix section.

To design a successful control strategy, a rotating reference frame has been considered in order to operate and control in a rotating dq-coordinate system. In this dq-reference frame, the torque equation for a Permanent Magnet Synchronous Machine (PMSM) is given (Dominguez, 2015) by (14):

$$T = 1.5\,P\left(\lambda_{pm}\,i_q + \left(L_d - L_q\right)i_d\,i_q\right) \qquad (14)$$

Where i_d and i_q are the direct and quadrature currents respectively. As in a SPMSM L_d and L_q have the same value (Skvarenina, 2002), Equation 14 can be rewritten as in (15):

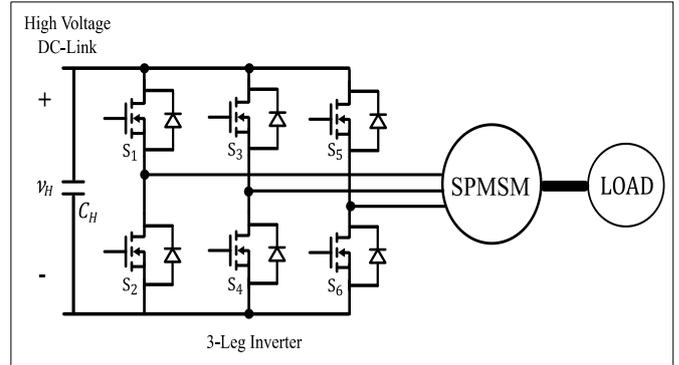$$T = 1.5\,P\,\lambda_{pm}\,i_q \qquad (15)$$

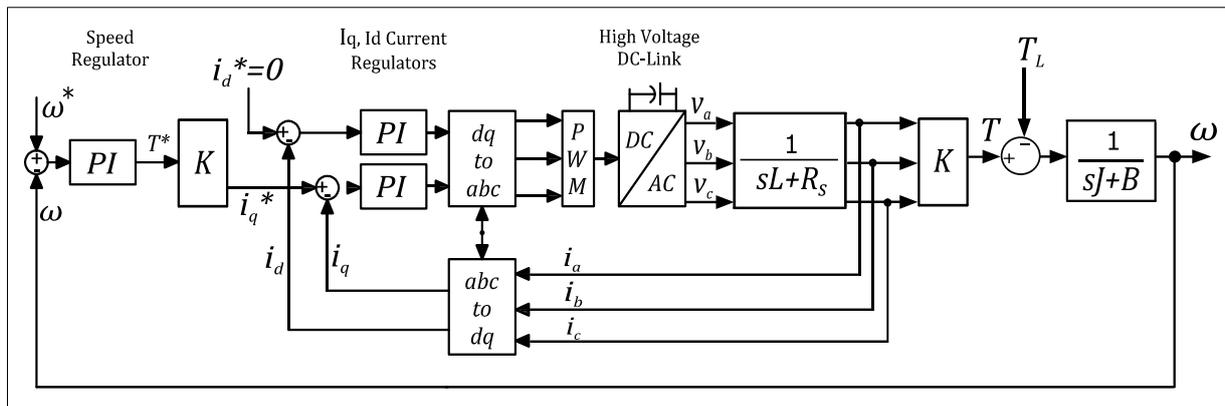**Figure 5**. Inverter and electric machine configuration

Figure 6. Cascade control scheme for the SPMSM

For electric traction applications, an outer superimposed speed controller is required where its output control signal is the torque reference for the inner current controller. To achieve this goal, a cascade control scheme is used as shown in Figure 6.

The inner control loop regulates the machine dq currents and the outer control loop regulates the machine angular speed ω provided that the mechanical time constant of the machine is much greater than the electrical time constant. As the torque reference can be obtained from the superimposed PI speed regulator (Drury, 2001), the required quadrature current reference (i_q^*) can then be found from Equation 15. On the other hand, the direct current reference (i_d^*) is set to be zero as the machine is a SPMSM. For the dq-current controllers, the selected closed-loop bandwidth ($BW_{d,q}$) was 500[Hz]. To obtain the PI parameters, Equations (16)-(17) were used.

$$Kp_{d,q} = 2\pi.BW_{d,q}.L_{d,q} \qquad (16)$$

$$Ti_{d,q} = L_{d,q}/R_s \qquad (17)$$

The methodology used to attain the PI parameters for the speed regulator is exposed in detail below. A similar procedure can be extended to the previously exposed controllers.

The torque-speed equation of the machine is as in (18):

$$\sum \mathrm{T} = T - T_L = J\frac{d}{dt}\omega + B\,\omega \qquad (18)$$

Being J, B and T_L the inertia of the shaft of the machine, the friction coefficient and the load torque respectively. Using the Laplace transform, the machine torque-speed transfer function $P(s)$ can be written as (19) details:

$$P(s) = \frac{\omega(s)}{T(s) - T_L(s)} = \frac{1}{Js + B} = \frac{\frac{1}{B}}{s\frac{J}{B} + 1} \qquad (19)$$

On the other hand, the transfer function of the PI controller for the speed regulator can be written as in (20):

$$C(s) = Kp_\omega\left(1 + \frac{1}{s\,T_{i_\omega}}\right) = Kp_\omega\left(\frac{s\,T_{i_\omega} + 1}{s\,T_{i_\omega}}\right) \quad (20)$$

Comparing Equations (19) and (20) and employing again the pole-cancellation principle for the design of the controller, Ti_ω is chosen according to (21):

$$Ti_\omega = J/B \qquad (21)$$

Therefore, the closed-loop transfer function $L(s)$ of the system is exposed in (22):

$$L(s) = \frac{P(s).C(s)}{1 + P(s).C(s)} = \frac{\frac{Kp_\omega}{Ti_\omega B}}{s + \frac{Kp_\omega}{Ti_\omega B}} = \frac{W_C}{s + W_C} \quad (22)$$

The previous expression can be related with a first order low-pass filter having a cut-off angular frequency W_C exhibited in (23):

$$W_C = 2\pi.BW_\omega \qquad (23)$$

Being BW_ω the closed-loop bandwidth for the speed controller which was chosen to be 100[Hz].
Considering Equations (21) to (23), Kp_ω can now be obtained as in (24):

$$Kp_\omega = 2\pi.BW_\omega.J \qquad (24)$$

4. DIGITAL IMPLEMENTATION

The digital PI controllers were implemented using the Tustin numerical integration exposed in (25):

$$U_k = U_{k-1} + q_0 e_k + q_1 e_{k-1} \qquad (25)$$

Where q_0 and q_1 relate to (26) and (27) respectively.

$$q_0 = K_p\left(\frac{T_c}{2T_i} + 1\right) \qquad (26)$$

$$q_1 = K_p\left(\frac{T_c}{2T_i} - 1\right) \qquad (27)$$

Being, U_k and e_k the actual variable value and its actual error, while U_{k-1} and e_{k-1} refer to the previous U_k value and error respectively. In addition, T_c stand for the sampling time and K_p and T_i for the PI parameters correspondingly. Regarding the simulation, PSIM® Software was used to setup the overall system: the bidirectional DC-DC power converter, the inverter, the SPMSM and the programmable mechanical load. After successful results were attained, all the control logic was digitally upgraded in the simulator for a Texas F28335 DSP using the SimCoder® add-on which generates all the C-code required to be directly programmed on the DSP to work properly. This option considerably reduces the prototyping process.

5. EXPERIMENTAL RESULTS

Suitable results were obtained after implementing the digital control for the bidirectional DC-DC converter as well as for the control of the SPMSM. Figure 7 shows in detail the results for the regulation of the DC-link voltage (v_H) besides the rotor speed (ω) that were successfully controlled according to the required references (v_H^*=500[V] and ω^*=1000[rpm]= 104.72[rad/s]) for motoring as well as for regeneration purposes, in one hand and on the other hand, the inductor current (i_L) is also appropriately regulated and flows from the battery to the SPMSM when the load torque (T_L^*) is positive and it flows from the electric machine to the battery when the load torque is negative, i.e. a regeneration condition. Figure 7b shows a magnifier of the i_d and i_q results, there it also can be checked that the quadrature

_____

current i_q (which is proportional to the torque) successfully follows the reference $i_q{}^*$ while the direct current i_d is controlled to zero.
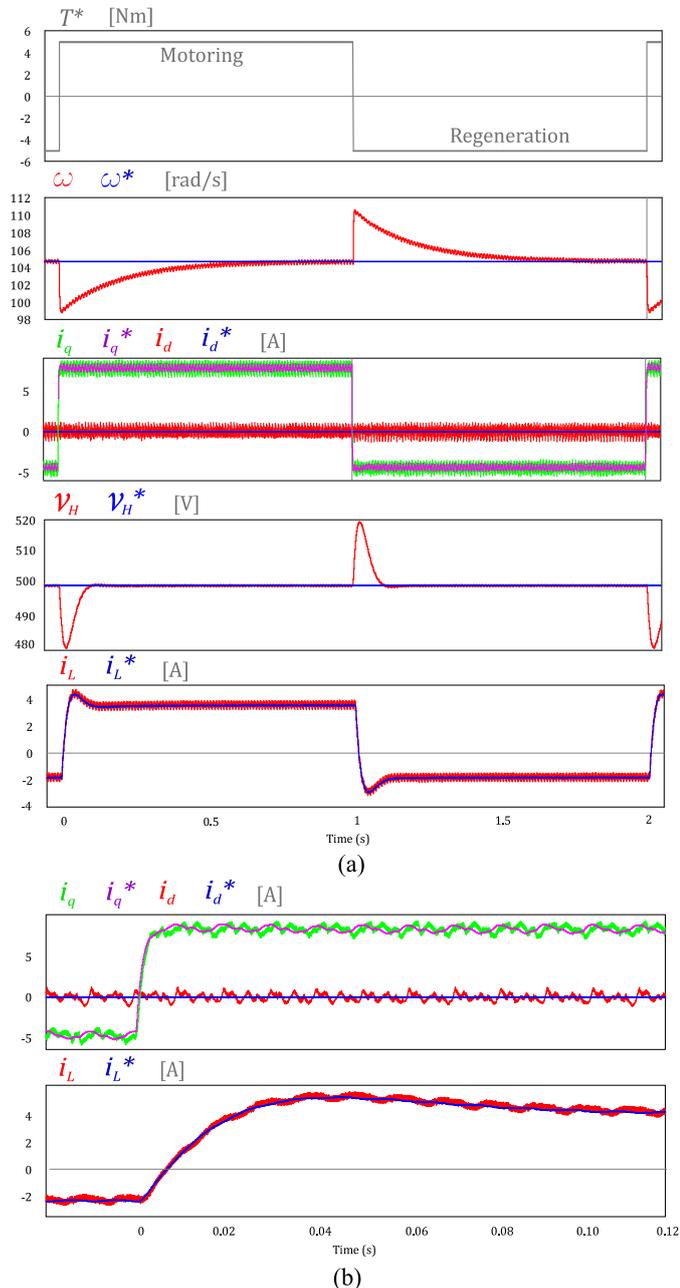

(a)

(b)

Figure 7. Experimental results: (a) Variables' response (b) Magnifier of the current responses

6. CONCLUSIONS

The power converters and the proposed control schemes involved an electric traction application have been designed and successfully verified. The control logic was developed to be directly run on a commercial embedded system. The proposed cascade control schemes in which PI-regulators were implemented, exhibited successful results when controlling the high-voltage DC link and the torque-speed regulation of the SPMSM by means of the vector control

strategy; suitable responses were attained for steady-state and during transients. The employed power topologies and control strategies proved to be a versatile solution for both operations: motoring and regeneration conditions.

APPENDIX

Table 1. SPMSM Data Sheets

Parameter	Symbol	Value
Stator resistance	R_S	435 [mΩ]
d- and q-axis stator inductance	L_d	3,95 [mH]
No-load peak line-to-line voltage constant	$Vpk/krpm$	98,67 [V] (peak value @ 1000[rpm])
Number of pole pairs	p	2
Moment of inertia	J	2,7E-3 [kg.m^2]
Rated current	I_n	10 [A]

REFERENCES

Dominguez, X. & Imbaquingo, C. (2015). Vector Control for an Interior Permanent Magnet Synchronous Machine with Maximum Torque per Ampere Strategy. *Revista Politécnica, Quito-Ecuador, Vol. 35*

Drury, B. (2001). *Control Techniques Drives and Control Handbook* (1st ed.). The Institution of Electrical Engineers

Du, Y., et al. (2010). Review of non-isolated bi-directional DC-DC converters for plug-in hybrid electric vehicle charge station application at municipal parking decks. *Applied Power Electronics Conference and Exposition (APEC),* 1145-1151

Erickson, R. & Maksimovi, D. (2001). *Fundamentals of Power Electronics* (2nd ed.). Springer

Junhong, Z., et al. (2008). Bidirectional DC-DC converter modeling and unified controller with digital implementation. *Applied Power Electronics Conference and Exposition APEC 2008.* 1747-1753

Kitajima, J. & Ohishi, K. (2014). Rapid and stable speed control of SPMSM based on current differential signal. *Power Electronics Conference (IPEC-Hiroshima 2014 - ECCE-ASIA),* 1247-1252

Maekawa, S., et al. (2014). Study of low speed sensorless drives for SPMSM by controlling elliptical inductance. *Power Electronics Conference (IPEC-Hiroshima 2014 - ECCE-ASIA),* 919-924

Pillay, P. & Krishnan, R. (1985). Control characteristics and speed controller design of a high performance PMSM, *IEEE Ind. Appl. Soc. Annual. Meeting*, 627-633.

Savaresi, M., et al. (2010). *Semi-Active Suspension Control Design for Vehicles* (1st ed.). Elsevier

Skvarenina, T. (2002). *The Power Electronics Handbook* (1st ed.). CRC Press

Tarakanath, K., et al. (2014). Internal model control of dc-dc boost converter exhibiting non-minimum phase behavior. *Drives and Energy Systems (PEDES), 2014 IEEE International Conference*, 1-7

Xavier Dominguez holds and Electronics and Control Engineering Degree from the Escuela Politécnica Nacional (Quito-Ecuador/2010) and a Master in Electrical Energy Conversion and Power Systems from the University of Oviedo (Gijón-Spain/2014) thanks to a Senescyt scholarship. Currently, he is an Assistant Professor at the Universidad Técnica del Norte (Ibarra-Ecuador). His interests are power converters, power quality, distributed generation and renewable energy design, planning and integration. (E-mail: exdominguez@utn.edu.ec)

Marcelo Pozo was born in Quito-Ecuador. In 1999 he obtained the Electronics and Control Engineering Degree at the Escuela Politécnica Nacional (Quito-Ecuador). In 2002 thanks to a DAAD scholarship he obtained the M.Sc. degree at the Dresden Technical University (Dresden-Germany). From 2003 to 2009 he gained expertise at the industry. Since 2009 he is a Principal Professor at the Escuela Politécnica Nacional in the Automation and Control Department (DACI). In 2015 he obtained the Doctoral Engineering degree in Power Electronics and Electrical Machine Control at the Siegen University (Germany). His interests are power electronics, energy efficiency, power quality, renewable energy and electrical vehicles. (Email: marcelo.pozo@epn.edu.ec)

Leonardo Ortega was born in Quito, Ecuador in 1985. He received the B.S. degree in Electronic Engineering from Escuela Politecnica Nacional - Ecuador in 2010 and the M.S. degree in Electrical, electronic and automatic engineering from Carlos III University of Madrid in 2013 thanks to a Senescyt scholarship. Currently, he is an Assistant Professor in the area of Power Electronics in the Escuela Politecnica Nacional. His research interests include power electronics, active filters and dc-dc converters with applications in renewable energy and smart grids. (E-mail: leonardo.ortega@epn.edu.ec).